Received: 30 May 2024 | Revised: 30 August 2024 | Accepted: 20 September 2024 | Published online: 25 September 2024

RESEARCH ARTICLE

Archives of Advanced Engineering Science
2024, Vol. 00(00) 1–13
DOI: 10.47852/bonviewAAES42023531

Spurious Accelerations in Finite Element Analysis of Geotechnical Problems: Cause and Remedy

Dhanaji Chavan[1],*

[1]*Department of Civil Engineering, Walchand College of Engineering Sangli, India*

Abstract: Present study investigates the response of the two distinct geotechnical problems under earthquake loading. These two problems are (1) nailed soil slope and (2) 1-D site response analysis. The aim of the study is to understand the cause of spurious accelerations and suggest a remedy. Two distinct interface conditions were considered in modeling the nailed soil slope. In first, the soil-nail interface was considered to be perfectly bonded. In second case, the sliding at the interface was allowed. The analysis resulted into the physically acceptable deformations. However, the dumbbell-shaped spurious acceleration pattern was observed in perfect bonding case. Further, the maximum acceleration was found to span from 4 g to 13 g. Such extremely high accelerations are unphysical and hence unacceptable. In case of 1-D site response analysis, misleading acceleration spike of magnitude twice that of true acceleration was noted. The introduction of the numerical damping successfully removed the spurious accelerations and resulted in physically acceptable response for both problems.

Keywords: spurious acceleration, displacement, earthquake loading, finite element analysis, damping

1. Introduction

Finite element analysis is widely used to model simple to complex problems in the field of geotechnical earthquake engineering [1–4]. Issues such as size of finite element, constitutive model, type of loading, and boundary conditions play vital role in the modeling [5, 6]. Another crucial factor that affects the dynamic response of the structure is damping [7]. When a material is subjected to dynamic loading and it undergoes plastic deformation, there is loss of energy. This loss of energy is called *material damping*. Because of the material damping, the stress-strain curve of the soil becomes hysteretic under cyclic/dynamic loading [8]. In numerical modeling such as finite element/finite difference method, the material damping is taken care of by the hysteretic constitutive model. Since in numerical analysis infinite domain is curtailed and represented as finite domain, the propagation of waves away from the domain is modeled with dampers which are usually dashpot. This is called as *radiation damping* [9]. Strictly speaking, these two are the only damping sources in the physical model. However, if we run analysis with the above two damping only, it is observed that the response obtained contains the spurious frequency components in the acceleration records. And to get the realistic response, artificial damping either in the form of *Rayleigh damping* or *Numerical damping* needs to be introduced. Hall [10] alarmed about the misuse of Rayleigh damping in the dynamic analysis of structures. He proposed bounds on the damping forces as the possible remedy. He felt need of further research in this area to avoid misuse of the damping. Sun and Dias [8] revealed that misuse of the Rayleigh damping significantly affects the response of the geotechnical structures such as tunnel. They found that, however, the due attention is conventionally not paid to this issue. Further, it was suggested that more than one analysis should be performed to gain the confidence in the results obtained. The research carried out so far has mostly focused on use/misuse of Rayleigh damping. Another damping which is artificially induced in the analysis is *Numerical damping*. Effect/side effect of this damping is yet to be explored especially in the dynamic analysis of geotechnical or soil-structure interaction problems.

It is worth to note that there is no hard and fast rule to define numerical damping. The present study sheds light on the significance of numerical damping in the finite element analysis of geotechnical problems. For this purpose, following two distinct problems are investigated: (1) nailed soil slope and (2) 1-D site response analysis.

2. Problem 1: Nailed Soil Slope

Reinforcing the existing slopes with nails is one of the widely adopted approaches to increase its stability under static and dynamic loading [11–14]. The stability analysis of such slopes is usually performed by following three methods: (1) Static: when only static load is considered, (2) Pseudo-static: when earthquake load is considered, and (3) Numerical modeling: used for static as well as dynamic loading [15]. It is believed that the solution obtained by numerical modeling is more rigorous and involved. Usually, finite difference method or finite element method is used to model the boundary value problem. Significant experimental, theoretical, and numerical research has been carried out so far on stability analysis of nailed slopes [16–21]. The research reveals that the performance of the slope is significantly enhanced on reinforcing it with the nails. Numerical analysis is pretty simple when only static load is considered. However, it becomes highly complicated when dynamic load such earthquake comes into the picture.

*Corresponding author: Dhanaji Chavan, Department of Civil Engineering, Walchand College of Engineering Sangli, India. Email: dhanaji.chavan@walchandsangli.ac.in

Figure 1
The geometry of nailed soil slope considered in the study

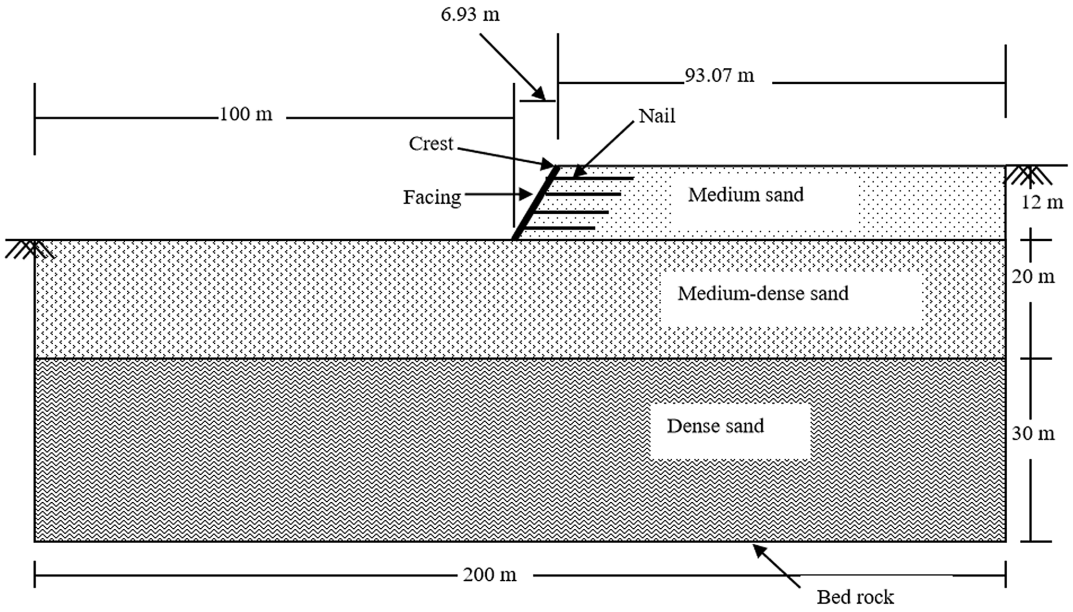

In the present study, a 60° nailed soil slope was modeled as a plane strain problem (Figure 1 [22]) and was subjected to the earthquake load, as shown in Figure 2, at the base. The analysis was carried out in an open-source software OpenSees [23, 24]. Nails are modeled with two noded beam element with three degrees of freedom at each node, *i.e.*, two translations and one rotation. Soil is modeled with four noded quad element with two degrees of freedom at each node, *i.e.,* X-translation and Y-translation. The mesh was fine in the nailed region and was coarser towards the boundary of the domain. Elements as small as 0.33 m × 0.40 were used in the nailed region. Dashpots were provided at the base and lateral boundaries to simulate radiation damping happening at the boundary. Further details about the points such as constitutive model for soil, interface modeling, boundary conditions etc., can be found in Chavan et al. [22]. Since the objective of the present paper is to discuss spurious response, above details are not repeated here for brevity. The verification and validation results are also given in the paper by Chavan et al. [22]. The 1940 Imperial Valley Earthquake record with PGA = 0.348 g, shown in Figure 2, is applied at the base of the model as input motion.

It is a well-established fact that when the actual domain is discretized, the artificial high-frequency components get introduced in the analysis. There is no well-established and unique approach to dampen out these high-frequency components [8, 10, 22, 25]. Generally, verification and validation of the model are performed to get confidence in the results obtained from the analysis. In the present study, verification was performed with SHAKE2000 and validation of nailed model was done with experimental work of Hong et al. [26]. In spite of the successful verification and validation, it was observed that the acceleration records obtained at the Toe and Crest of the slope were extremely high, physically unbelievable and hence unacceptable.

Following remedies were tried to remove these spurious accelerations: (1) incorporating Rayleigh damping and (2) introducing numerical damping. Out of these two approaches, first approach did not work, whereas second approach was found to be effective. Rayleigh damping is mostly used to induce small strain damping in the analysis, and it comprises stiffness proportional terms and mass proportional terms. Ineffectiveness of the Rayleigh damping in removing spurious accelerations needs further research.

Figure 2
The input acceleration record for nailed slope

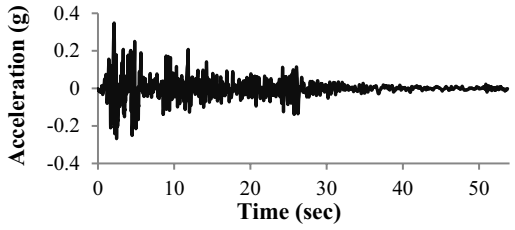

2.1. Results and discussion for nailed slope

The analysis was performed for two distinct interface conditions: (1) NoSS: No Sliding and Separation at the soil-nail interface. This represents perfect bonding condition; (2) SS: Sliding and Separation at the soil-nail interface is allowed. The acceleration response obtained from the analysis at the Toe and Crest of the slope is shown in Figures 3 to 6. Figures 3 and 4 show horizontal acceleration response, and Figures 5 and 6 show vertical acceleration response at Toe and Crest, respectively.

In Figure 3a, peculiar dumbbell-shaped acceleration pattern is observed for NOSS case. Further, the acceleration as high as 4 g is noted. In case of SS, the horizontal acceleration at Toe is observed to be as high as 11.02 g. The corresponding acceleration amplification is 32. Thus, both acceleration and amplification are enormous and unbelievable. The maximum horizontal acceleration observed at Crest in NOSS case is around 2.6 g and in SS case around 7.38 g. Again, these accelerations are significantly high

Figure 3
Horizontal acceleration records at Toe: (a) NoSS case and (b) SS case

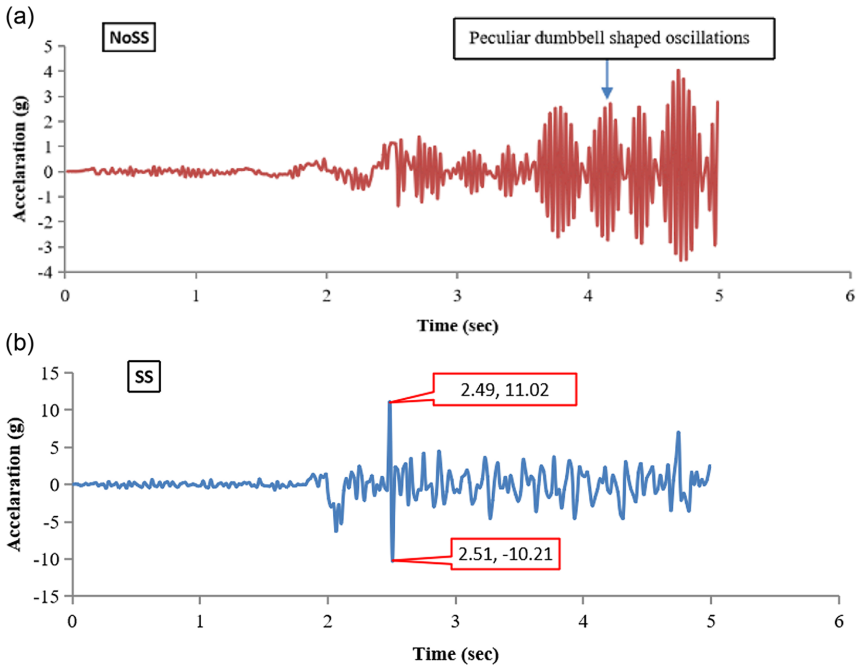

Figure 4
Horizontal acceleration records at Crest: (a) NoSS case and (b) SS case

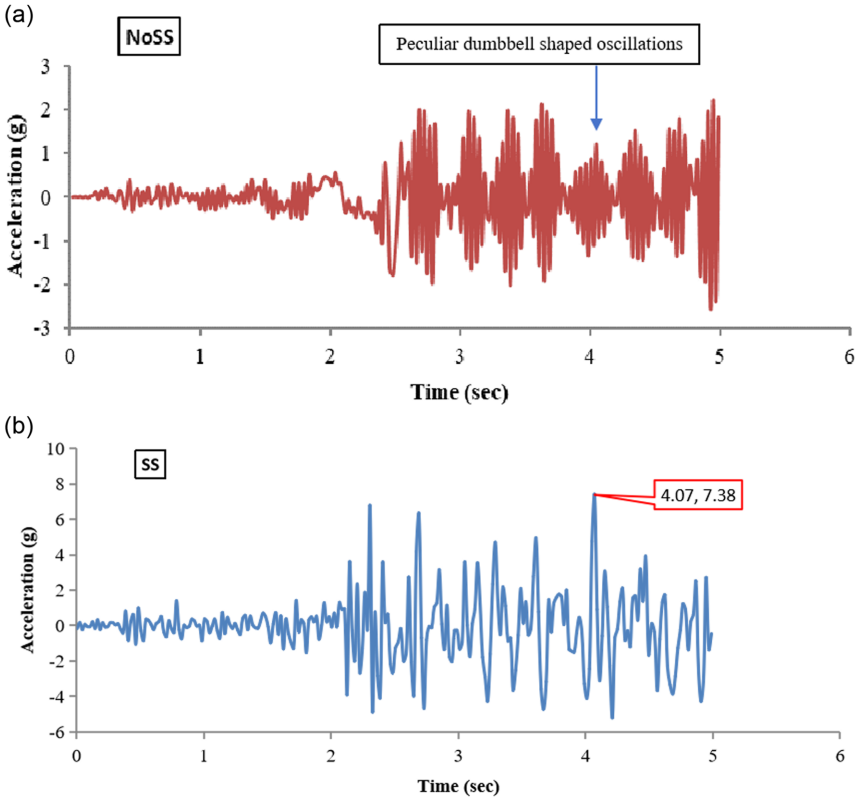

Figure 5
Vertical acceleration records at Toe: (a) NoSS case and (b) SS case

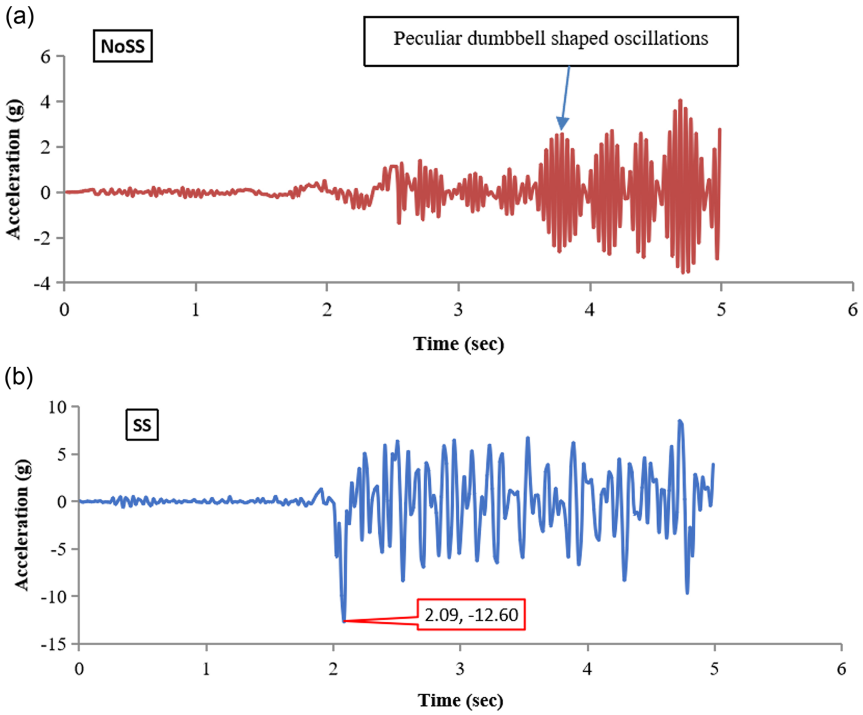

Figure 6
Vertical acceleration records at Crest (a) NoSS case and (b) SS case

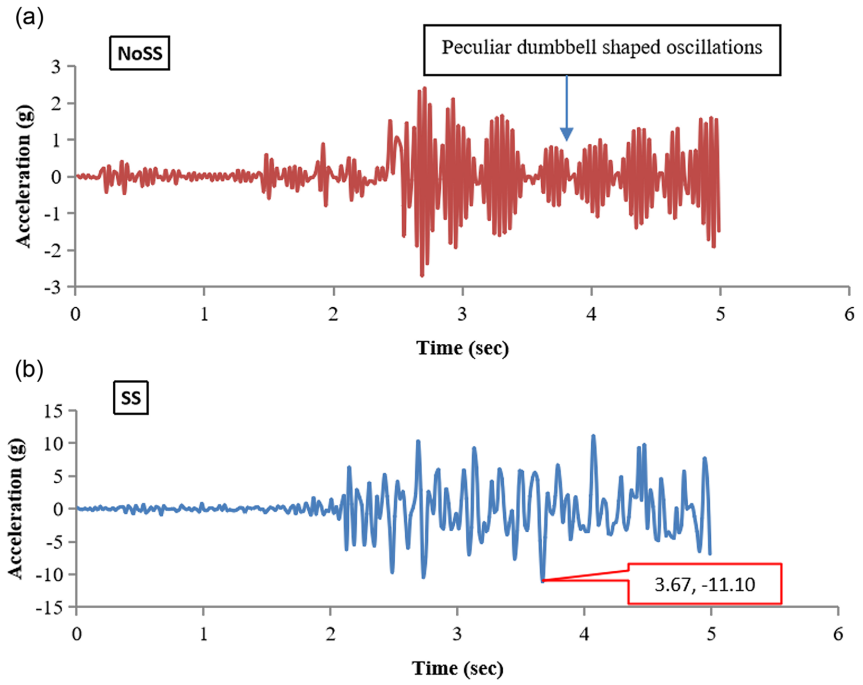

Figure 7
Corrected horizontal acceleration at Toe: (a) NoSS case and (b) SS case

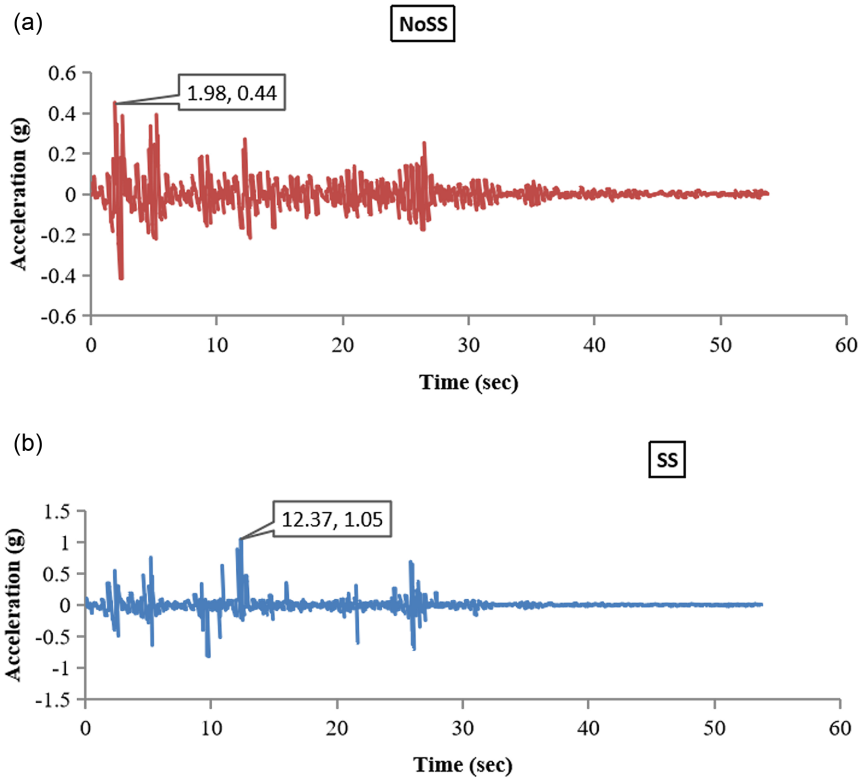

Figure 8
Corrected horizontal accelerations at Crest: (a) NoSS case and (b) SS case

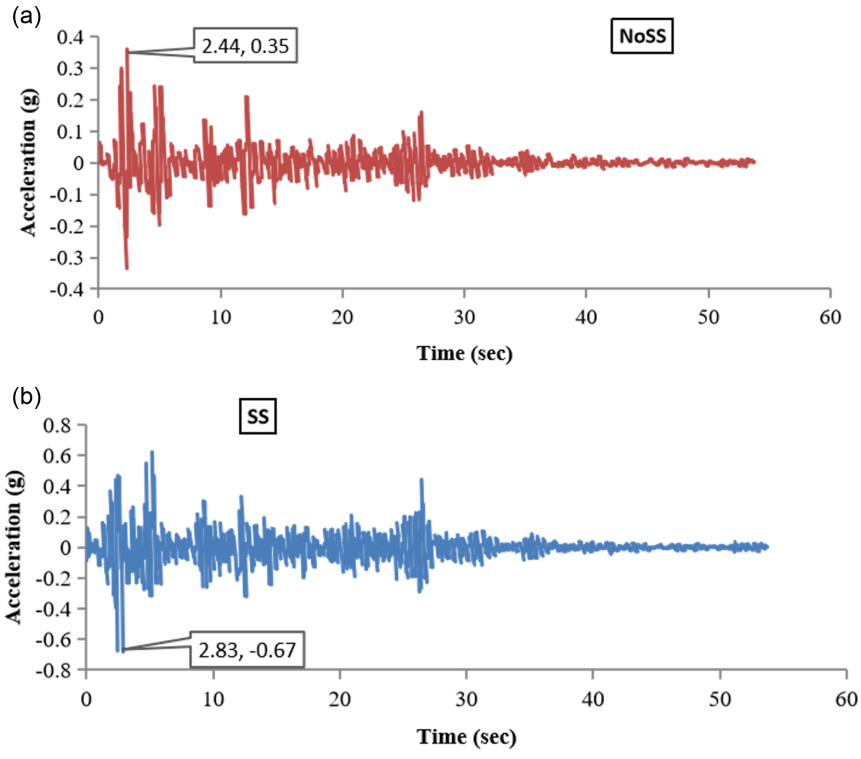

Figure 9
Corrected vertical accelerations at Toe: (a) NoSS case and (b) SS case

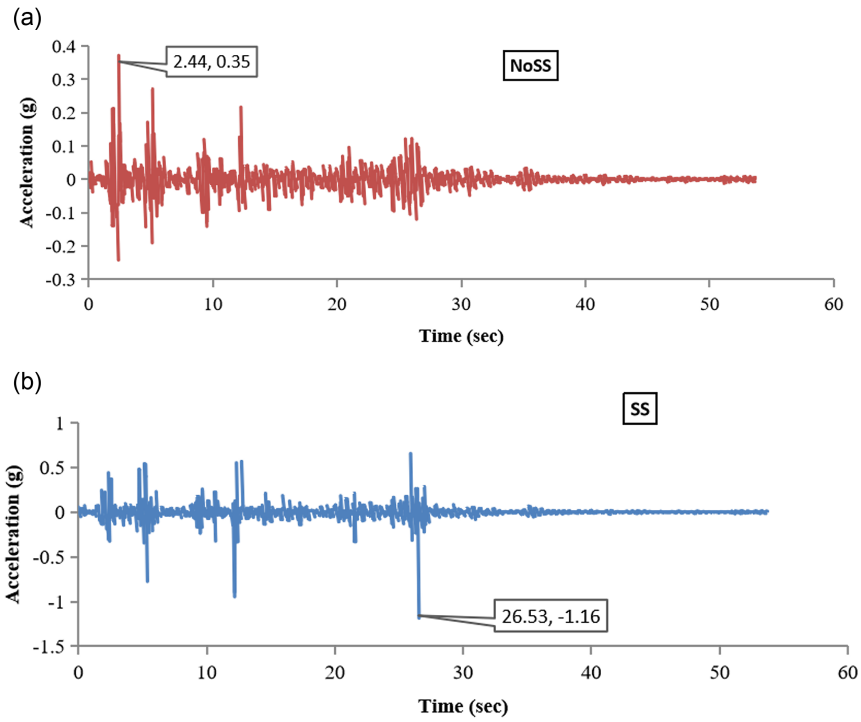

Figure 10
Corrected vertical accelerations at Crest: (a) NoSS case and (b) SS case

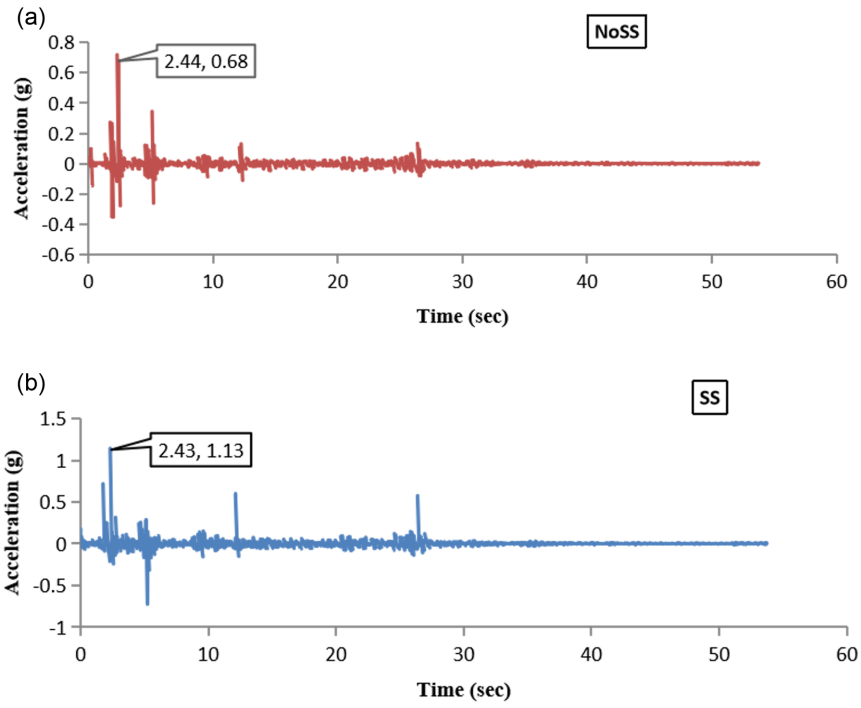

Figure 11
Comparison of horizontal displacement before and after application of numerical damping at: (a) Toe and (b) Crest

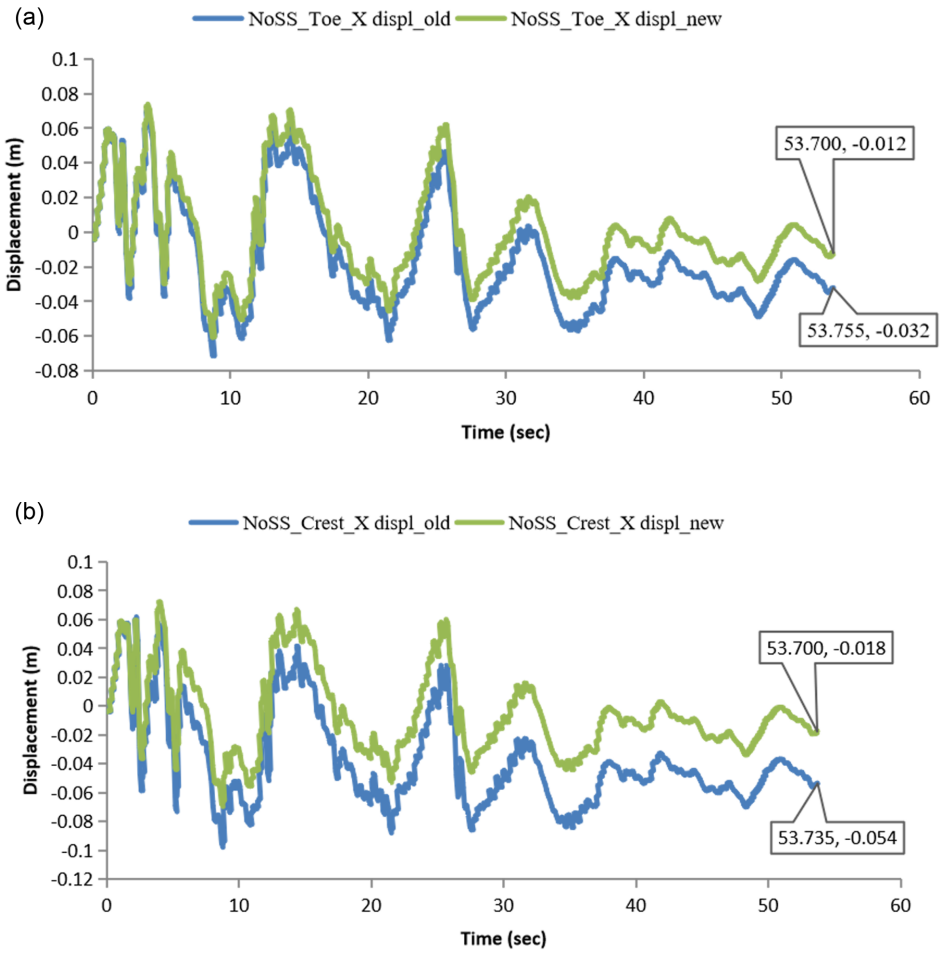

and practically unbelievable. It is worth to note here, from Figures 3 and 4, that the peculiar dumbbell-shaped pattern is observed for NoSS case only and is absent for SS case. This implies that the perfect bonding condition at nail and soil interface is responsible for this dumbbell-shaped pattern. This condition is imposed at the soil-nail interface by employing equal degree of freedom constraint in x and y direction.

The vertical acceleration response at the Toe and Crest is shown in Figures 5 and 6, respectively. Again it is observed that the peculiar dumbbell-shaped pattern prevails. At Toe, the maximum vertical acceleration is noticed to be around 12.6 g and 4 g for NoSS and SS case, respectively. In Figure 6, the maximum vertical acceleration at the Crest is found to be around 2.7 g and 11.10 g for NoSS and SS case, respectively.

It is worth noting that only horizontal input acceleration was applied, and this should have ideally resulted in amplified horizontal accelerations only. However, the vertical acceleration as high as 12.6 g was observed in the present analysis. Moreover, the vertical accelerations are found to be greater than the horizontal acceleration. Again it is worth to note that the peculiar dumbbell-shaped pattern is shown by both horizontal and vertical records of the NoSS case.

In reality, just few cycles of the horizontal acceleration in the range of 5 g to 10 g would induce extremely high shear stresses in the structure such as nailed slope, retaining wall, and cause complete failure of such structures. However, in the present analysis, the deformation of slope was observed to be very small and there was no complete failure as such. Also, there is no field evidence of such huge accelerations and amplifications that would cause total destruction of soil-nailed structures.

It should be noted that the above accelerations existed even after the successful validation of the finite element model with the shake table studies of Hong et al. [26]. The normalized facing displacement obtained from the finite element analysis, for SS case, was found to be in good agreement with the one experimentally observed by Hong et al. [26].

To look into the abovementioned spurious accelerations, several simulations were performed. At the end, it was found that these records were due to time integration technique used for the nonlinear seismic analyses. The time integration method used in the analyses was the Newmark method. This is the most widely used method with γ (gamma) parameter as 0.5 and β (beta) parameter as 0.25 (these are the default values). The equations used for this method are given below:

Figure 12
Comparison of vertical displacement before and after application of the numerical damping at: (a) Toe and (b) Crest

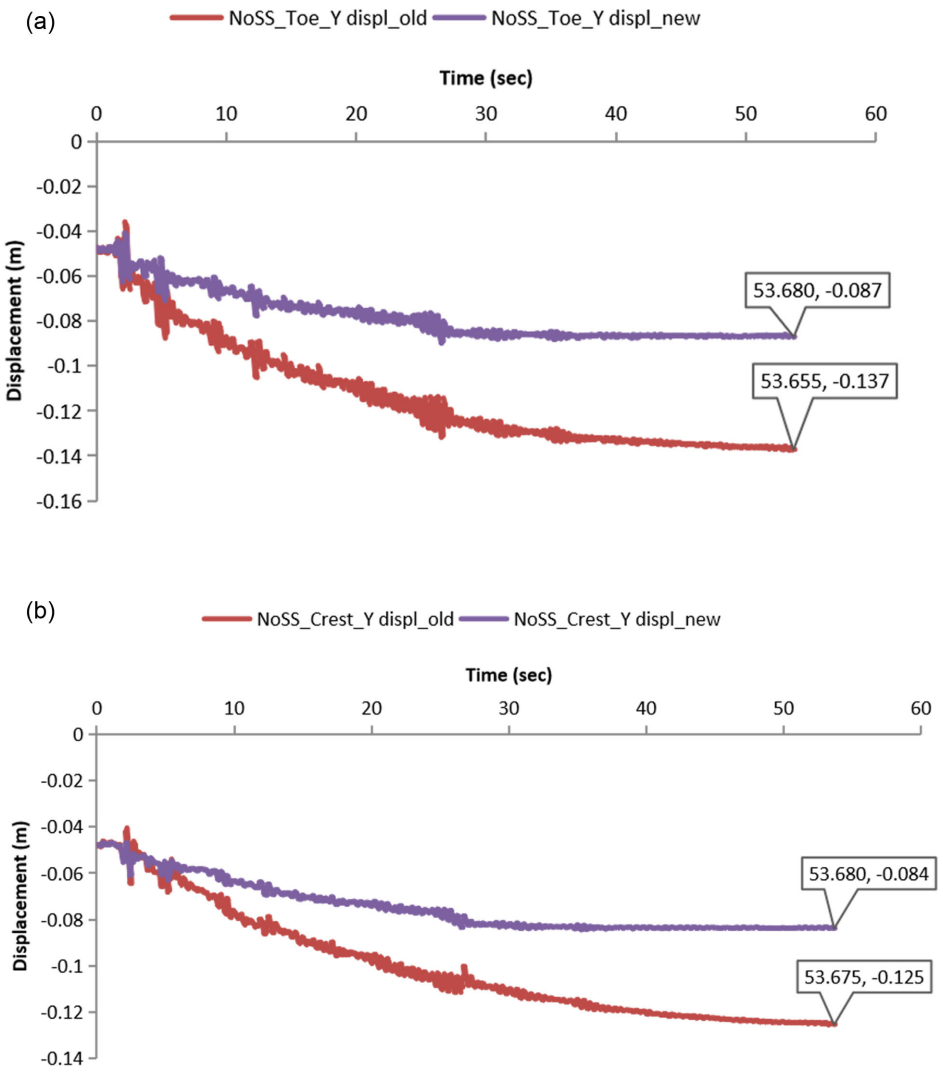

$$M\ddot{u}_t + C\dot{u}_t + Ku_t = F_t \tag{1}$$

$$\dot{u}_t = \dot{u}_{(t-\Delta t)} + (1-\gamma)\Delta t\ddot{u}_{(t-\Delta t)} + \gamma(\Delta t)\ddot{u}_t \tag{2}$$

$$u_t = u_{(t-\Delta t)} + \Delta t\dot{u}_{(t-\Delta t)} + \left(\frac{1}{2} - \beta\right)(\Delta t)^2\left(\ddot{u}_{(t-\Delta t)}\right) + \beta(\Delta t)^2\ddot{u}_t \tag{3}$$

where M is the mass matrix, C is the damping matrix, K is the stiffness matrix, F_t is the external force at time t; $\ddot{u}_t$, $\dot{u}_t$, and u_t are the acceleration, velocity, and displacement at time t, Δt is the time step. The Equations (1), (2), and (3) are solved iteratively for each time step for each displacement degree of freedom. Acceleration is obtained from Equation (1).

The Newmark method with default values of gamma and beta failed to remove the high-frequency spurious accelerations in the analysis. In the end, it was realized that to remove the artificial higher frequency accelerations components, a numerical damping needs to be introduced adopting unconditional stable criteria given in Equation (4) [27].

For $0 \leq \xi < 1$,

$$\gamma \geq \tfrac{1}{2}$$

$$\beta \geq \left(\frac{\gamma + \frac{1}{2}}{4}\right)^2 \tag{4}$$

Authors performed several simulations according to this rule and found that for values of $\gamma = 1$ and $\beta = 0.5625$, the spurious accelerations are damped out. The corrected acceleration records are shown in the Figures 7 to 10. From Figure 7a it is observed that dumbbell-shaped erroneous acceleration pattern is completely removed and maximum acceleration is 0.35 g which is significantly less than that observed before application of numerical damping (i.e., 4 g). The spurious acceleration also got removed from the SS acceleration record as seen in Figure 7b. The maximum acceleration observed in this case is 1.05 g which is again significantly less than that observed before

Figure 13
Mesh considered in the analysis of 1-D site response

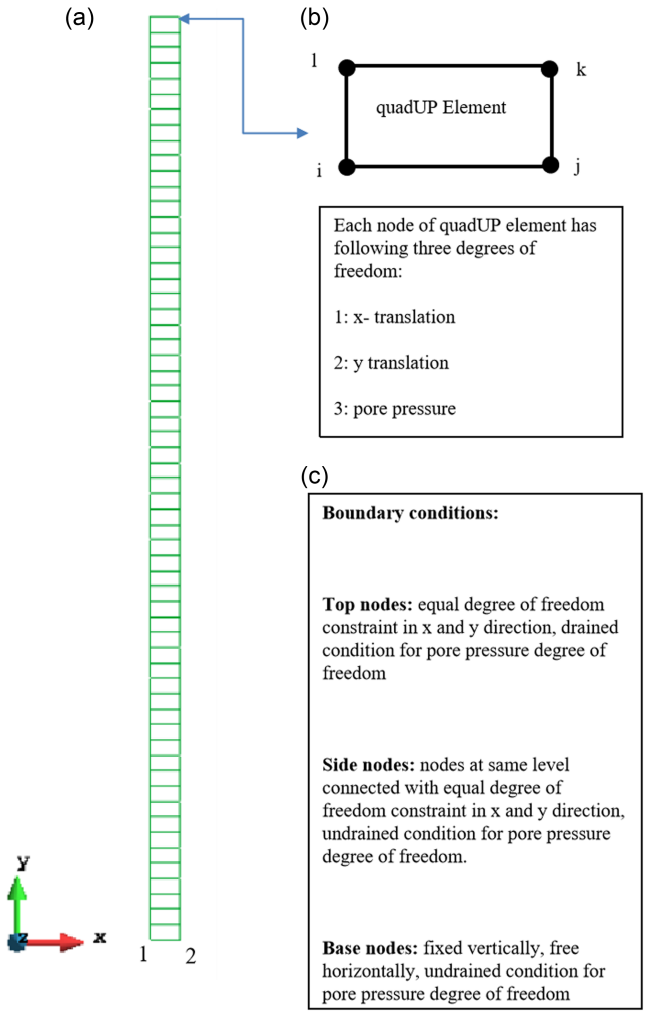

application of the numerical damping (*i.e.,* 11 g). Observation of the Figures 8 to 10 reveals that numerical damping has been effective in removing the spurious high magnitude acceleration components.

To check how much is the change in the displacements, the displacements at the Toe and Crest have been plotted from old analysis and corrected one (new). The plots are shown in the Figures 11 and 12. From Figure 11a, it is observed that the old and new horizontal displacements of the Toe are identical up to 26 s. Beyond this time, they differ in magnitudes. However, it is interesting to note that the pattern of the displacement evolution is identical in both cases. The displacement observed at the end of analysis is −0.012 m and −0.032 m for new and old case, respectively. Thus, application of numerical damping reduced the horizontal displacement at the end of the analysis; however, the pattern of displacement evolution remained unaffected.

The horizontal displacement of the Crest at the end of analysis is observed to be −0.018 m and −0.054 m for new and old case, respectively. Thus, the new displacement is almost one-third of the old displacement. Figure 12 shows vertical displacement of the Toe and Crest. It is observed that pattern of displacement evolution remains same in old and new case. Further, application of the numerical damping reduced the vertical displacement at the end of analysis.

3. Problem 2: 1-D Site Response Analysis

Site response analysis of the ground is one of the conventional problems in the field of geotechnical earthquake engineering. Most of the time, this analysis is performed as 1 – dimensional assuming only vertical propagation of horizontal shear wave. The domain is then discretized as shown in Figure 13 [28]. The domain shown in the Figure 13 [28] comprises four node quadrilateral element called as quadUP. The formulation of the element is based on the plain strain assumption. As shown in the Figure 13, each node has three degrees of freedom: first two degrees of freedom are translational and third one is pore pressure. The pore pressure degree of freedom captures the development of pore water pressure during monotonic or cyclic undrained loading. The element works on the Biot's theory of poro-elasticity. The stress-strain response of the soil is modeled using pressure dependent multi-yield material model present in the OpenSees.

The domain is assumed to be homogenous and made up of medium dense sand with saturated unit weight of 1.98 t/m^3, friction angle 34°, phase transformation angle 26.5°, and initial void ratio 0.684. Advanced material properties of the sand considered in the analysis are given in Chavan et al. [28].

The input motion is applied at the base and response of the ground in the form of displacement, and acceleration is obtained. In this section, 1-D site response with and without application of the numerical damping is investigated. Details of the constitutive model, boundary conditions, etc., can be found in Chavan et al. [28].

To ascertain the accuracy of the finite element analysis results, usually verification is performed. Verification ensures that the mathematical formulation is working correctly, and the results obtained from the analysis are reliable. One of the approach is comparing the results obtained from finite elements analysis with the closed form/analytical/so-called exact solution if available. Another approach is comparing results obtained from one software with the results obtained from another software for the same model. First approach is possible for only simple problems where geometry is regular and the material stress-strain response is either linear elastic. When the geometry is irregular or the soil stress-strain response is highly nonlinear and plastic, the closed form/analytical solution is almost absent. Again, second approach is trustworthy only when the problem to be modelled is simple. In the present study, author has tried very simple but innovative approach. And this approach is based on the fundamental understanding that the input acceleration or velocity or displacement applied at the base node of the model must match the acceleration/velocity/displacement record obtained from the analysis for that node. Though this sounds trivial, it is worth to note that the two records, i.e., input and one obtained from analysis, match only when the simulation results are correct for the entire domain. This argument is proved in this section and the remedy is suggested when the analysis is erroneous.

In the present study, input motion is applied at the base node in the form of equivalent nodal shear force. For this purpose, input acceleration record was first converted into velocity record and then the equivalent nodal shear force (F) was computed from the following equation:

$$F = v_i \rho v_s A \tag{5}$$

Figure 14
Comparison of the input acceleration and acceleration obtained from analysis for gamma 0.5 and beta 0.25 case: (a) Input acceleration, (b) comparison between input and analysis acceleration, and (c) Enlarged view to detail spurious accelerations

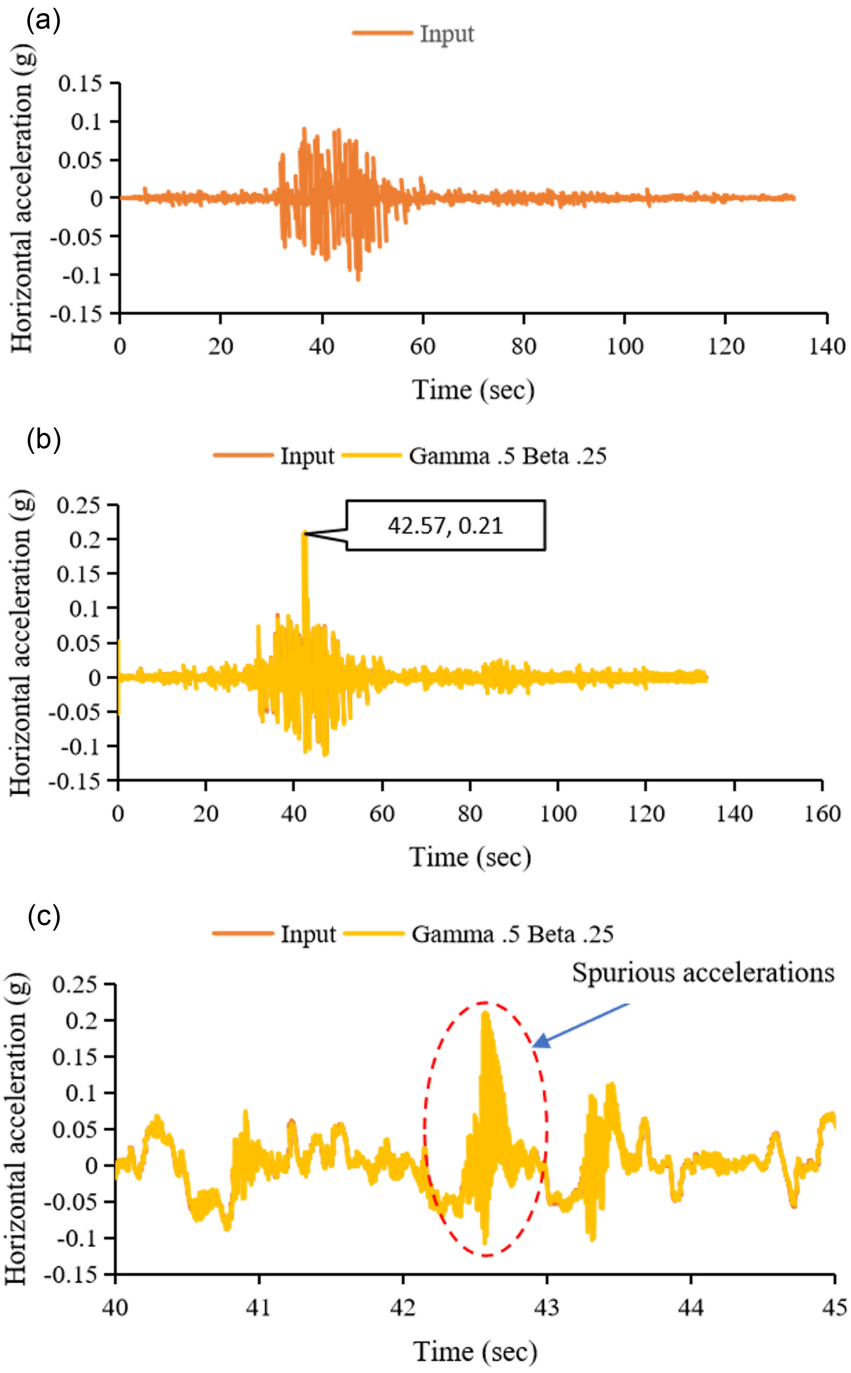

where v_i is input velocity, ρ is mass density of the bedrock (in present study 2.5 t/m^3), v_s is the shear wave velocity of the bedrock (in present study 700 m/s), A is tributary nodal area (in present study 1 m^2). The equivalent nodal shear force given by Equation (5) is applied at the base node.

In the present study, Bhuj 2001, N78E component, recorded at the Ahmedabad station has been used as input motion. Its duration is 133.53 s, and peak acceleration is 0.106 g. At the base node, motion is applied in the form of equivalent shear force. Software takes this as the input and computes the acceleration, velocity, and displacement at all nodes in the finite element domain. It calculates these parameters at the base node also. *The acceleration computed at the base node must be equal to the acceleration applied as input since at a node there cannot be two acceleration values at a given time*. This is applicable to velocity and displacement response as well. The input velocity, displacement, and acceleration records

Figure 15
(a) Comparison of input acceleration with acceleration obtained from analysis for gamma 0.7 and beta 0.35; (b) enlarged view showing removal of spurious acceleration

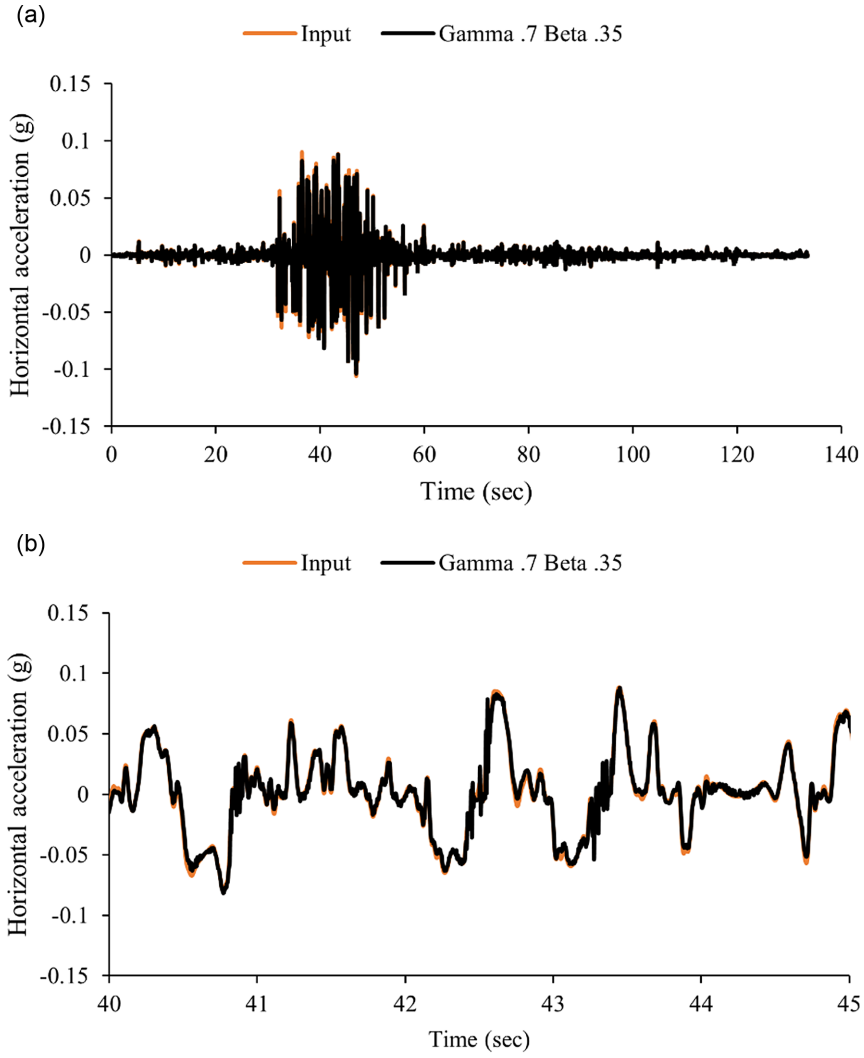

were compared with those obtained from the finite element analysis at the base node. The input acceleration record is shown in the Figure 14a. The comparison between the acceleration records is shown in Figure 14b for Newmark integration scheme having gamma 0.5 and beta 0.25. It is observed that the acceleration obtained from the analysis contains spurious high-frequency components. It is seen that the spike of 0.21 g at 42.57 s observed in the Figure 14b is spurious one. It should be noted that these spurious acceleration components are consequence of the finite element discretization and are not present in real physical system. To remove these spurious components, gamma and beta were chosen to be 0.7 and 0.35. This introduces the numerical damping and removes the spurious high-frequency components as shown in the Figure 15. It should be noted that the values of the gamma and beta were arrived at after performing several trial simulations. From the enlarged view of the acceleration records shown in Figure 15b, it is clear that the spurious acceleration components are completely removed. From this figure, it is observed that there is an excellent agreement between the input acceleration record and acceleration record obtained from the finite element analysis. The comparison between displacement and velocity records is also shown in Figure 16, and excellent agreement is found between input record and analysis record. This implies that the results generated by the finite element analysis are correct and hence acceptable.

Figure 16
Comparison of input displacement and velocity with those obtained from analysis

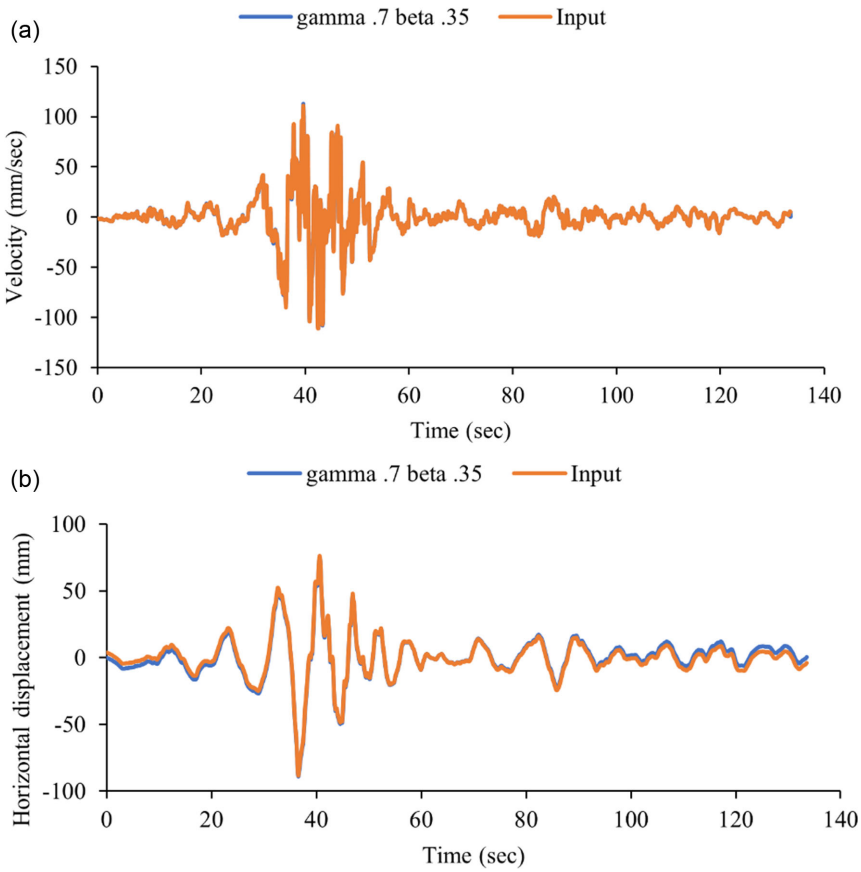

4. Conclusions

Two distinct cases of finite element analysis of the geotechnical earthquake engineering problem are discussed in this paper. The peculiar dumbbell-shaped acceleration pattern, in nailed slope case, was attributed to the perfect bonding condition at the soil-nail interface. The finite element discretization introduced spurious acceleration as high as 12 g in the analysis. When the numerical damping was introduced following unconditionally stable criteria, it was observed that all spurious acceleration components got damped out. The maximum acceleration noted after introduction of numerical damping was 1.16 g, though high it is acceptable. Effect of numerical damping on displacement (which in turn causes deformation) was also investigated. It is found that numerical damping reduces the displacement; however, pattern of displacement evolution remains unaffected.

In case of 1-D site response analysis, it was observed that application of numerical damping removed the high-frequency spurious accelerations.

5. Recommendations

Many real life geotechnical problems need dynamic analysis. The finite element discretization of such problems may induce erroneous accelerations. Generally, high-frequency spikes observed in the acceleration response are due to the numerical discretization of the model and needs to be removed to get the realistic response. From the present study, it is recommended that appropriate numerical damping should be introduced in the finite element analysis of geotechnical problems to damp out the spurious acceleration and displacement response and to get the realistic response of the structure.

Ethical Statement

This study does not contain any studies with human or animal subjects performed by any of the authors.

Conflicts of Interest

The author declares that he has no conflicts of interest to this work.

Data Availability Statement

Data available on request from the corresponding author upon reasonable request.

Author Contribution Statement

Dhanaji Chavan: Conceptualization, Methodology, Software, Validation, Formal analysis, Investigation, Resources, Data curation, Writing – original draft, Writing – review & editing.

References

[1] Carbonell, J. M., Monforte, L., Ciantia, M. O., Arroyo, M., & Gens, A. (2022). Geotechnical particle finite element method for modeling of soil-structure interaction under large

deformation conditions. *Journal of Rock Mechanics and Geotechnical Engineering*, *14*(3), 967–983. https://doi.org/10.1016/j.jrmge.2021.12.006

[2] Deng, P., Liu, Q., Huang, X., & Ma, H. (2021). A new hysteretic damping model and application for the combined finite-discrete element method (FDEM). *Engineering Analysis with Boundary Elements*, *132*(June), 370–382. https://doi.org/10.1016/j.enganabound.2021.08.021

[3] Guan, Q. Z., Yang, Z. X., Guo, N., & Hu, Z. (2023). Finite element geotechnical analysis incorporating deep learning-based soil model. *Computers and Geotechnics*, *154*, 105120. https://doi.org/10.1016/j.compgeo.2022.105120

[4] Liu, J., Wu, L., Yin, K., Song, C., Bian, X., & Li, S. (2022). Methods for solving finite element mesh-dependency problems in geotechnical engineering—A review. *Sustainability (Switzerland)*, *14*(5), 1–20. https://doi.org/10.3390/su14052982

[5] Liu, Z., Qiao, Y., Cheng, X., & El Naggar, M. H. (2022). Nonlinear seismic response and amplification effect of 3D sedimentary basin based on bounding surface constitutive model. *Soil Dynamics and Earthquake Engineering*, *158*, 107292. https://doi.org/10.1016/j.soildyn.2022.107292

[6] Onyelowe, K. C., Ebid, A. M., Ramani Sujatha, E., Fazel-Mojtahedi, F., Golaghaei-Darzi, A., Kontoni, D. P. N., & Nooralddin-Othman, N. (2023). Extensive overview of soil constitutive relations and applications for geotechnical engineering problems. *Heliyon*, *9*(3), e14465. https://doi.org/10.1016/j.heliyon.2023.e14465

[7] Mijatović, O., Borković, A., Guzijan-Dilber, M., Mišković, Z., Salatić, R., Mandić, R., & Golubović-Bugarski, V. (2023). Experimental and numerical study of structural damping in a beam with bolted splice connection. *Thin-Walled Structures*, *186*, 110661. https://doi.org/10.1016/j.tws.2023.110661

[8] Sun, Q., & Dias, D. (2018). Significance of Rayleigh damping in nonlinear numerical seismic analysis of tunnels. *Soil Dynamics and Earthquake Engineering*, *115*, 489–494. https://doi.org/10.1016/j.soildyn.2018.09.013

[9] Ambrosini, R. D. (2006). Material damping vs. radiation damping in soil–structure interaction analysis. *Computers and Geotechnics*, *33*(2), 86–92. https://doi.org/10.1016/j.compgeo.2006.03.001

[10] Hall, J. F. (2006). Problems encountered from the use (or misuse) of Rayleigh damping. *Earthquake Engineering and Structural Dynamics*, *35*(5), 525–545. https://doi.org/10.1002/eqe.541

[11] Chavan, D., Mondal, G., & Prashant, A. (2012). Permanent displacement of nailed soil slopes subjected to earthquake loading. In *Proceedings of the 15th World Conference on Earthquake Engineering*, *35*, 27755–27762.

[12] Cheuk, C. Y., Ng, C. W. W., & Sun, H. W. (2005). Numerical experiments of soil nails in loose fill slopes subjected to rainfall infiltration effects. *Computers and Geotechnics*, *32*(4), 290–303. https://doi.org/10.1016/j.compgeo.2005.02.005

[13] Mohamed, M. H., Ahmed, M., Mallick, J., & AlQadhi, S. (2023). Finite element modeling of the soil-nailing process in nailed-soil slopes. *Applied Sciences (Switzerland)*, *13*(4), 2139. https://doi.org/10.3390/app13042139

[14] Patra, C. R., & Basudhar, P. K. (2005). Optimum design of nailed soil slopes. *Geotechnical and Geological Engineering*, *23*(3), 273–296. https://doi.org/10.1007/s10706-004-2146-7

[15] Kramer, S. L. (1996). *Geotechnical earthquake engineering*. India: Prentice-Hall of India Private Limited.

[16] Fan, C. C., & Luo, J. H. (2008). Numerical study on the optimum layout of soil-nailed slopes. *Computers and Geotechnics*, *35*(4), 585–599. https://doi.org/10.1016/j.compgeo.2007.09.002

[17] Giri, D., & Sengupta, A. (2009). Dynamic behavior of small scale nailed soil slopes. *Geotechnical and Geological Engineering*, *27*(6), 687–698. https://doi.org/10.1007/s10706-009-9268-x

[18] Maleki, M., Khezri, A., Nosrati, M., & Hosseini, S. M. M. M. (2023). Seismic amplification factor and dynamic response of soil-nailed walls. *Modeling Earth Systems and Environment*, *9*, 1181–1198. https://doi.org/10.1007/s40808-022-01543-y

[19] Rawat, S., & Gupta, A. K. (2016). Analysis of a nailed soil slope using limit equilibrium and finite element methods. *International Journal of Geosynthetics and Ground Engineering*, *2*(4), 1–23. https://doi.org/10.1007/s40891-016-0076-0

[20] Tei, K., Taylor, R. N., & Milligan, G. W. E. (1998). Centrifuge model tests of nailed soil slopes. *Soils and Foundations*, *38*(02), 165–177. https://www.jstage.jst.go.jp/article/bpb1993/17/11/17_11_1460/_pdf/-char/ja

[21] Wei, W. B., & Cheng, Y. M. (2010). Soil nailed slope by strength reduction and limit equilibrium methods. *Computers and Geotechnics*, *37*(5), 602–618. https://doi.org/10.1016/j.compgeo.2010.03.008

[22] Chavan, D., Prashant, A., & Mondal, G. (2017). Seismic analysis of nailed soil slope considering interface effects. *Soil Dynamics and Earthquake Engineering*, *100*, 480–491. https://www.sciencedirect.com/science/article/pii/S0267726117306528

[23] Mazzoni, S., Mckenna, F., Scott, M. H., & Fenves, G. L. (2009). *OpenSees command language manual*. Retrieved from: https://opensees.berkeley.edu/OpenSees/manuals/usermanual/index.html

[24] Pacific Earthquake Engineering Research Center. (2016). *Open System for Earthquake Engineering Simulation, version 2.5.0*. Retrieved from: http://opensees.berkeley.edu/OpenSees/user/download.php

[25] Broderick, B. M., Elnashai, A. S., & Izzuddin, B. A. (1994). Observations on the effect of numerical dissipation on the nonlinear dynamic response of structural systems. *Engineering Structures*, *16*(1), 51–62. https://doi.org/10.1016/0141-0296(94)90104-X

[26] Hong, Y. S., Chen, R. H., Wu, C. S., & Chen, J. R. (2005). Shaking table tests and stability analysis of steep nailed slopes. *Canadian Geotechnical Journal*, *42*(5), 1264–1279. https://doi.org/10.1139/t05-055

[27] Hughes, T. J. (2000). *The finite element method: Linear static and dynamic finite element*. USA: Prentice-Hall, Inc. https://doi.org/10.1111/j.1467-8667.1989.tb00025.x

[28] Chavan, D., Sitharam, T. G., & Anbazhagan, P. (2022). Site response analysis of liquefiable soil employing continuous wavelet transforms. *Geotechnique Letters*, *12*(1), 1–11. https://doi.org/10.1680/jgele.21.00091

How to Cite: Chavan, D. (2024). Spurious Accelerations in Finite Element Analysis of Geotechnical Problems: Cause and Remedy. *Archives of Advanced Engineering Science*. https://doi.org/10.47852/bonviewAAES42023531